



This is a repository copy of *The effect of metal-rich growth conditions on the microstructure of ScxGa1-xN films grown using molecular beam epitaxy.*

White Rose Research Online URL for this paper:
<http://eprints.whiterose.ac.uk/93558/>

Version: Accepted Version

Article:

Tsui, H.C.L., Goff, L.E., Barradas, N.P. et al. (7 more authors) (2015) The effect of metal-rich growth conditions on the microstructure of ScxGa1-xN films grown using molecular beam epitaxy. *physica status solidi (a)*, 212 (12). 2837 - 2842. ISSN 1862-6300

<https://doi.org/10.1002/pssa.201532292>

Reuse

Unless indicated otherwise, fulltext items are protected by copyright with all rights reserved. The copyright exception in section 29 of the Copyright, Designs and Patents Act 1988 allows the making of a single copy solely for the purpose of non-commercial research or private study within the limits of fair dealing. The publisher or other rights-holder may allow further reproduction and re-use of this version - refer to the White Rose Research Online record for this item. Where records identify the publisher as the copyright holder, users can verify any specific terms of use on the publisher's website.

Takedown

If you consider content in White Rose Research Online to be in breach of UK law, please notify us by emailing eprints@whiterose.ac.uk including the URL of the record and the reason for the withdrawal request.



eprints@whiterose.ac.uk
<https://eprints.whiterose.ac.uk/>

The effect of metal-rich growth conditions on the microstructure of $\text{Sc}_x\text{Ga}_{1-x}\text{N}$ films grown using molecular beam epitaxy

H. C. L. Tsui¹, L. E. Goff^{1,2}, N. P. Barradas³, E. Alves^{4,5}, S. Pereira⁶, H. E. Beere², I. Farrer², C. A. Nicoll², D. A. Ritchie², M. A. Moram¹

¹Dept. Materials, Imperial College London, Exhibition Road, London SW7 2AZ, UK

²Dept. Physics, University of Cambridge, JJ Thomson Avenue, Cambridge CB3 0HE, UK

³C²TN - Centro de Ciências e Tecnologias Nucleares, Instituto Superior Técnico, Universidade de Lisboa, E.N. 10 ao km 139,7, 2695-066 Bobadela LRS, Portugal

⁴IPFN - Instituto de Plasmas e Fusão Nuclear, Av. Rovisco Pais, 1049-001 Lisboa, Portugal

⁵Laboratório de Aceleradores e Tecnologias de Radiação, Instituto Superior Técnico, Universidade de Lisboa, E.N. 10 ao km 139,7, 2695-066 Bobadela LRS, Portugal

⁶CICECO and Dept. of Physics, Universidade de Aveiro, 3810-193 Aveiro, Portugal

Abstract

Epitaxial $\text{Sc}_x\text{Ga}_{1-x}\text{N}$ films with $0 \leq x \leq 0.50$ were grown using molecular beam epitaxy under metal-rich conditions. The $\text{Sc}_x\text{Ga}_{1-x}\text{N}$ growth rate increased with increasing Sc flux despite the use of metal-rich growth conditions, which is attributed to the catalytic decomposition of N_2 induced by the presence of Sc. Microstructural analysis showed that phase-pure wurtzite $\text{Sc}_x\text{Ga}_{1-x}\text{N}$ was achieved up to $x = 0.26$, which is significantly higher than that previously reported for nitrogen-rich conditions, indicating that the use of metal-rich conditions can help to stabilise wurtzite phase $\text{Sc}_x\text{Ga}_{1-x}\text{N}$.

Keywords: ScGaN, molecular beam epitaxy, TEM

PACS codes: 61.66Dk, 68.55Nq, 81.05Ea, 81.15Hi

1 Introduction Wurtzite-structure III-nitrides are of interest for optoelectronic and high power electronic applications. These semiconductors include AlN, GaN and InN and their alloys, which have direct band gaps of 6.2 eV, 3.4 eV and 0.7 eV respectively [1–4] and are therefore able to emit light across the ultraviolet, violet and red spectral regions. However, current state-of-the-art optoelectronic devices suffer from poor internal quantum efficiencies, partly due to the lattice mismatch with the substrate or between layers leading to high dislocation densities and in-plane stresses [5]. Therefore, it is of interest to develop new wurtzite-structure nitride semiconductors with different lattice parameter-band gap relationships, such as alloys between GaN and ScN.

ScN is stable in the cubic rock-salt structure with an a lattice constant of 4.51 Å [6] while GaN favours the hexagonal wurtzite structure with an a lattice constant of 3.189 Å and c lattice constant of 5.185 Å [7]. ScN is of interest in its own right as an electronic and thermoelectric material [8–14] and as a dislocation reduction layer in GaN heterostructures [15–18]. The structural stability of different phases of ScN and $\text{Sc}_x\text{Ga}_{1-x}\text{N}$ has been investigated by theoretical calculations [19–22]. ScN has been predicted to be metastable in a non-polar hexagonal-BN-like structure with a c/a lattice parameter ratio of 1.207 and a u parameter of 0.515. Experimental stabilisation of this phase is of particular interest as it is predicted to be associated with the appearance of highly strain-tunable band gaps and ferroelectric properties [22,23]. Zhang et al. predicted that $\text{Sc}_x\text{Ga}_{1-x}\text{N}$ prefers the polar

wurtzite structure up to $x = 0.66$, where the c/a lattice parameter ratio will decrease until a h-BN-like phase appears, after which a phase transition to the rock salt structure should occur [22]. However, spinodal decomposition may occur as x increases. For example, $\text{Sc}_x\text{Ga}_{1-x}\text{N}$ has been predicted to be stable in the wurtzite phase only up to $x = 0.27$, if it is strained to GaN [16]. However, it is well known that non-equilibrium phases can be stabilised for the case of thin films using molecular beam epitaxy (MBE) [24]. Therefore, experimental growth of $\text{Sc}_x\text{Ga}_{1-x}\text{N}$ across a range of different conditions is required to determine what can be stabilised in practice.

$\text{Sc}_x\text{Ga}_{1-x}\text{N}$ has already been produced by sputtering [25], resulting in amorphous films, and molecular beam epitaxy (MBE) using plasma-activated N_2 [26] or NH_3 [27] as a nitrogen source, resulting in epitaxial films. Constantin et al. grew $\text{Sc}_x\text{Ga}_{1-x}\text{N}$ films under nitrogen-rich conditions using N_2 activated with an RF plasma source and found the following structures: wurtzite-like for $x \leq 0.17$, mixed-phase for $0.17 < x < 0.54$ and rock-salt for $x \geq 0.54$. The c/a ratio was found to decrease linearly with increasing x for the samples in the wurtzite-like regime, consistent with the predictions by Farrer et al. and Zhang et al. [22,23,26]. Moram et al. grew films using MBE under nitrogen-rich conditions using NH_3 as a nitrogen source, obtaining wurtzite-structure films for $0 < x < 0.08$ [27,28]. However, no reports exist for the growth of $\text{Sc}_x\text{Ga}_{1-x}\text{N}$ under metal-rich conditions, even though these conditions are known to produce GaN films with smoother surfaces and lower defect densities compared to GaN grown under nitrogen-rich conditions [29–32]. Therefore, this report investigates the growth and microstructure of $\text{Sc}_x\text{Ga}_{1-x}\text{N}$ films grown using MBE with metal-rich conditions.

2 Experimental methods Epitaxial $\text{Sc}_x\text{Ga}_{1-x}\text{N}$ films were grown on (0001)-oriented sapphire substrates with an in situ grown GaN buffer layer using MBE with an N_2 plasma source under metal-rich growth conditions. A layer of molybdenum (Mo) was deposited on the back of the sapphire substrate by sputtering to assist substrate temperature measurement using an optical pyrometer. The substrate temperature was kept at $750\text{ }^\circ\text{C}$ during growth of all layers. The film compositions were controlled by varying the Sc flux by adjusting the effusion cell temperature while maintaining a constant Ga flux, as measured using a beam flux monitor. The N_2 purity was 99.9999% (plus an in-line filter was used), the Ga purity was 99.9995% and the Sc purity was 99.999%. The Sc metal was purified by an electron beam refinement process, without using any fluorinated compounds at any stage of the purification, and thus no detectable fluorine was found in the target (in contrast to most commercially available Sc metal which is typically contaminated with fluorine). The N_2 chamber pressure was maintained at 8.5×10^{-5} mbar and the N plasma power was at 350 W. Prior to the 1 hr $\text{Sc}_x\text{Ga}_{1-x}\text{N}$ film growth, a GaN buffer layer was first deposited under the same conditions as the $\text{Sc}_x\text{Ga}_{1-x}\text{N}$ film on the substrate for 1 hr. The film thicknesses for $\text{Sc}_x\text{Ga}_{1-x}\text{N}$ range between 760 nm and 915 nm while the thickness for the GaN buffer layer is 650 nm. The film thicknesses were measured from the cross-sectional TEM images. Wet etching experiments also reveal that the MBE-grown GaN buffer layers are N-polar.

Rutherford backscattering (RBS) was carried out for film composition determination at 2 MeV with 4He with an incident angle of 0° , enabling $\text{Sc}_x\text{Ga}_{1-x}\text{N}$ composition determination to a precision of $x \pm 0.01$. Further details of composition determination will be published elsewhere [33]. A standard detector at 140° and two pin-diode detectors at 165° were placed in the RBS chamber. The RBS data analysis was performed using the IBA DataFurnace NDF v9.6d [34]. Surface morphology characterisation was performed using a Bruker Innova atomic force microscope (AFM) in tapping mode using a tip with a radius of 10 nm. AFM data analysis was carried out using WSxM software [35]. Raman spectroscopy was

performed using a HORIBA Jobin Yvon LabRAM HR800 Ev with a 532 nm laser, a 10x objective and a 1800 gr/mm grating. Conventional and high-resolution (HR) transmission electron microscopy (TEM) imaging was carried out using a JEOL 2000 and a JEOL 2100 microscope operating at 200 kV. High angle annular dark field (HAADF) imaging in the scanning transmission electron microscopy (STEM) mode was done using JEOL 2100 microscope. Cross-sectional and plan-view TEM samples were prepared by mechanical grinding followed by ion polishing. Energy dispersive X-ray spectroscopy (EDX) was performed using an Oxford instruments X-MaxN 80 silicon drift detector operated in a JEOL 2100 microscope.

3 Results and discussions

3.1 $\text{Sc}_x\text{Ga}_{1-x}\text{N}$ film growth rate The $\text{Sc}_x\text{Ga}_{1-x}\text{N}$ film growth rate was found to increase as the Sc flux increased and was 15%–30% higher than that of GaN grown under metal-rich conditions (Figure 1(a)). This increased growth rate can be attributed to the catalytic decomposition of N_2 by Sc, which has been reported previously for the case of ScN growth: ScN films can be grown directly from N_2 , without using a N_2 plasma source [36] (a plasma source is necessary for GaN growth, due to the insufficient reactivity of N_2 with Ga [37]). This effect is confirmed in our reactor for the case of pure ScN growth under conditions comparable to those used for $\text{Sc}_x\text{Ga}_{1-x}\text{N}$ growth, except that the N_2 plasma source was not switched on (Figure 1(b)). However, this catalytic effect leads to uncertainty regarding the true metal-to-nitrogen ratio at the growth surface. For instance, under metal-rich growth conditions, the GaN growth rate is limited by the supply of active N. Yet, in the case of $\text{Sc}_x\text{Ga}_{1-x}\text{N}$, the growth rate increases with increasing Sc flux, suggesting that additional active nitrogen has become available, alongside the increased total metal flux. Therefore additional evidence is needed to determine whether the films were grown in the metal-rich or nitrogen-rich growth regime.

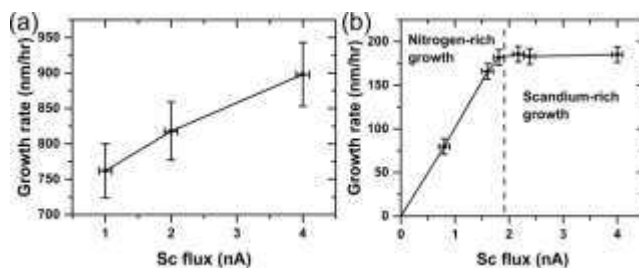


Figure 1 (a) Plot of the growth rates of wurtzite-structure $\text{Sc}_x\text{Ga}_{1-x}\text{N}$ as a function of Sc flux and (b) Plot of the ScN growth rate as a function of Sc flux with a N_2 gas flow rate of 1 sccm (no N_2 plasma source used).

3.2 $\text{Sc}_x\text{Ga}_{1-x}\text{N}$ film surface morphology Surface morphology measurements showed that the $\text{Sc}_x\text{Ga}_{1-x}\text{N}$ films become smoother as the Sc content increases (root-mean-square (RMS) roughness for $x = 0$ is 8.5 nm and $x = 0.26$ is 2.59 nm), due to a decrease in the average lateral feature size, until a phase transition to the rock salt structure occurs (RMS roughness for $x = 0.5$ is 19.05 nm). A similar trend has been demonstrated for MBE-grown films of MnGaN [38] and ScGaN [21] and is attributed to the decrease in surface adatom mobility due to an increase in the average diffusion barrier height with increasing surface concentrations of Mn and Sc respectively. These data also help to confirm that the films are grown under metal-rich conditions. The AFM image of GaN (Figure 2(a)) is consistent with growth under metal-rich conditions, as expected. Moreover, the morphologies of $\text{Sc}_x\text{Ga}_{1-x}\text{N}$

films for $0 \leq x \leq 0.26$ are comparable to those of MnGaN grown under the Ga-poor metal-rich regime in Ref. [38]. Therefore, we conclude that these films were grown under metal-rich conditions. The higher roughnesses found for the high Sc content $\text{Sc}_x\text{Ga}_{1-x}\text{N}$ film (Figure 2(f)) are most likely due to the presence of relatively large inclusions having the rock-salt crystal structure.

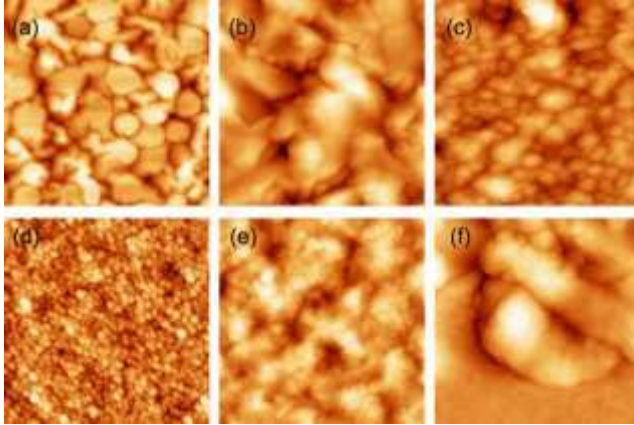


Figure 2 $1 \times 1 \mu\text{m}$ AFM images of $\text{Sc}_x\text{Ga}_{1-x}\text{N}$ films with increasing Sc content: (a) $x = 0$ (Z-scale = 58 nm), (b) $x = 0.08$ (Z-scale = 106 nm), (c) $x = 0.15$ (Z-scale = 70 nm), (d) $x = 0.26$ (Z-scale = 20 nm), (e) $x = 0.38$ (Z-scale = 27 nm), (f) $x = 0.50$ (Z-scale = 132 nm). All images were processed using parabolic flattening.

3.3 $\text{Sc}_x\text{Ga}_{1-x}\text{N}$ films microstructure and electron diffraction pattern The TEM data indicate that all films have a columnar microstructure (Figure 3). A similar columnar structure has been reported in both GaN [39,40] and ScN [41], however, a relatively high angle of 15° was observed between the ScN growth direction and the [0001] direction. At low Sc contents ($x = 0.08$ and $x = 0.15$), several superimposed diffraction patterns were observed in cross-section, indicating relative in-plane rotational misorientations of the grains. Moreover, consideration of the individual diffraction patterns from each grain showed that these $\text{Sc}_x\text{Ga}_{1-x}\text{N}$ films have hexagonal symmetry and are oriented in the [0001] direction out of plane, as confirmed by X-ray diffraction. However, at higher Sc contents (e.g. $x = 0.26$), there are two main relative in-plane rotational orientations of the hexagonal grains, as shown in the plan-view TEM images (Figure 4(a)). It is confirmed from the electron diffraction patterns that the in-plane rotation only occurs in $\text{Sc}_x\text{Ga}_{1-x}\text{N}$ film whereas there is no sign of rotation in the GaN buffer layer (Figure 4(b)). This relative in-plane rotation may occur to relieve the larger in-plane lattice mismatch between $\text{Sc}_x\text{Ga}_{1-x}\text{N}$ and GaN for films with higher Sc contents [42].

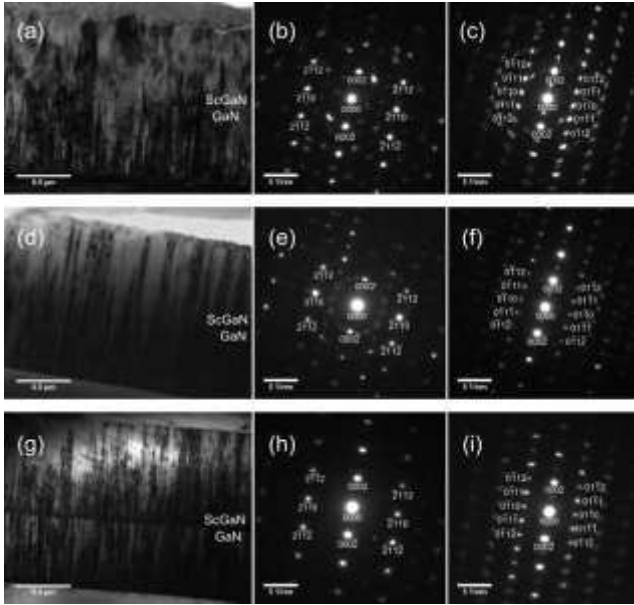


Figure 3 Cross-sectional bright field TEM images of hexagonal $\text{Sc}_x\text{Ga}_{1-x}\text{N}$ films obtained from the $\langle 01\bar{1}0 \rangle$ zone axis with (a) $x = 0.08$, (d) $x = 0.15$, (g) $x = 0.26$, with corresponding diffraction patterns obtained from (b), (e), (h) the $\langle 01\bar{1}0 \rangle$ $\text{Sc}_x\text{Ga}_{1-x}\text{N}$ zone axis and (c), (f), (i) the $\langle \bar{2}110 \rangle$ $\text{Sc}_x\text{Ga}_{1-x}\text{N}$ zone axis.

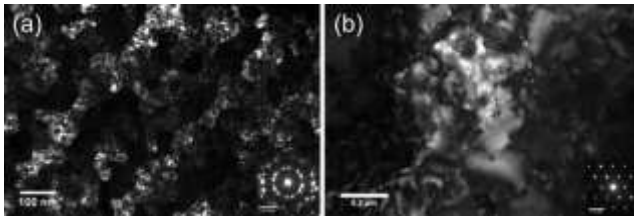


Figure 4 (a) Plan-view dark field TEM image of a hexagonal $\text{Sc}_x\text{Ga}_{1-x}\text{N}$ film with $x = 0.26$, with imaging conditions chosen to highlight regions of the film having only one of the two main in-plane orientations, insert: plan-view selected area diffraction pattern obtained from the same film; (b) plan-view dark field image of a GaN film grown under the same condition as the GaN buffer layer, insert: plan-view selected area diffraction pattern.

The c/a lattice parameter ratios of the hexagonal $\text{Sc}_x\text{Ga}_{1-x}\text{N}$ films were calculated from the electron diffraction patterns. The c/a ratio of the $\text{Sc}_x\text{Ga}_{1-x}\text{N}$ film decreased from 1.61 to 1.57 as the Sc content increased from $x = 0.08$ to $x = 0.26$. The result was consistent with previous theoretical and experimental data indicating that the c/a ratio decreases as the Sc content increases [22,26]. The reference c/a ratios of the GaN layer calculated from the diffraction patterns averaged 1.625 ± 0.005 , in good agreement with literature values [43–45]. This indicates that, under metal-rich conditions, $\text{Sc}_x\text{Ga}_{1-x}\text{N}$ in the pure wurtzite phase can be achieved up to $x = 0.26$, which agrees with the theoretical values precisely [21,22].

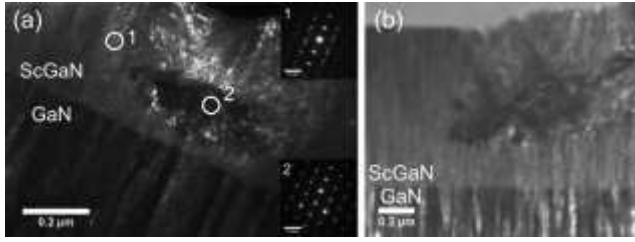


Figure 5 (a) Cross-sectional dark field TEM images of a $\text{Sc}_x\text{Ga}_{1-x}\text{N}$ film with $x = 0.50$. White circles indicate the locations from which the diffraction patterns in the insets (1) and (2) were taken; (b) $\text{Sc}_x\text{Ga}_{1-x}\text{N}$ twinned grains with the rock-salt structure formed near the film surface.

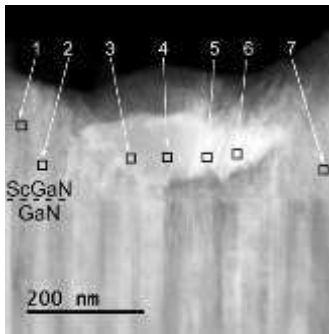


Figure 6 STEM HAADF image of a $\text{Sc}_x\text{Ga}_{1-x}\text{N}$ film with $x = 0.50$ (black squares indicate the points where EDX measurements were carried out).

Table 1 Sc contents (x) measured using energy-dispersive X-ray spectroscopy (EDX) for a $\text{Sc}_x\text{Ga}_{1-x}\text{N}$ film with overall $x = 0.50$ at the points indicated in Figure 6.

Point	x (Sc content)
1 (hexagonal)	0.56
2 (hexagonal)	0.55
3 (cubic)	0.69
4 (cubic)	0.62
5 (cubic)	0.90
6 (cubic)	0.95
7 (hexagonal)	0.55

However, mixed hexagonal and cubic phases are observed for films with Sc contents $x > 0.26$, as indicated by selected area diffraction patterns obtained in cross section (Figure 5). The hexagonal regions of the film have a similar columnar microstructure to the films with lower Sc contents. In contrast, the cubic regions of the film have relatively large, rounded grains. The diffraction patterns obtained from these regions are consistent with the fcc rock-salt structure (e.g. the fcc [011] pattern shown in Figure 5(a), inset 2). Some twinning was also observed within the cubic regions (Figure 5(b)). The STEM HAADF showed a relative increase in the Sc content within the cubic inclusions (Figure 6), as confirmed by energy-dispersive X-ray spectroscopy (EDX) analysis performed on both the hexagonal and the cubic parts of the films (Table 1). This suggests that phase decomposition may have occurred and/or that Sc droplets (which subsequently became nitrided) may have accumulated on the surface of the films having such high Sc contents ($x = 0.5$). Considering the RBS measurement as a reference, the Sc concentration measured using EDX on the hexagonal

regions is slightly higher than that measured using RBS. In spite of the measurement error of EDX, the Sc concentration at the cubic parts appears higher than that at the hexagonal parts.

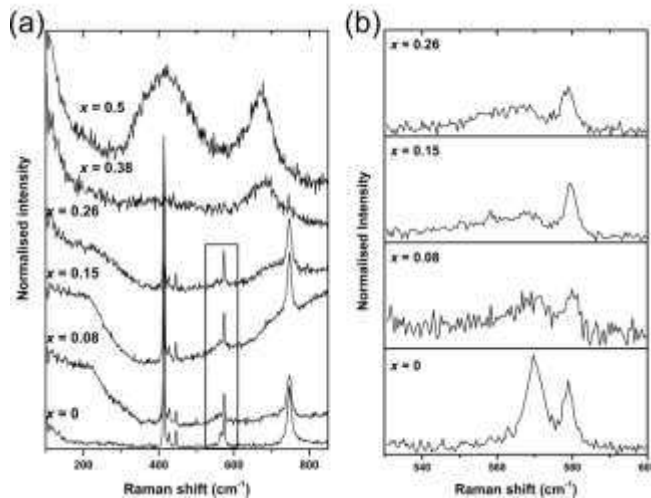


Figure 7 (a) Raman spectra for GaN and $\text{Sc}_x\text{Ga}_{1-x}\text{N}$ films; (b) shows the E_2^H phonon mode of GaN and $\text{Sc}_x\text{Ga}_{1-x}\text{N}$ films, enlarged from the boxed area in (a).

3.4 Raman spectrum from $\text{Sc}_x\text{Ga}_{1-x}\text{N}$ films The observed trends in the Raman spectra are also consistent with the microstructural changes observed in TEM. The peak associated with the E_2^H phonon mode of the wurtzite phase disappears when x increases from 0.26 to 0.38, confirming the presence of a phase transition from phase-pure wurtzite films to mixed-phase or purely cubic films (Figure 7(a)). The broad peaks at 400 and 670 cm^{-1} obtained from $\text{Sc}_{0.38}\text{Ga}_{0.62}\text{N}$ and $\text{Sc}_{0.5}\text{Ga}_{0.5}\text{N}$ are believed to be the phonon modes from ScN [46,47]. The presence of mixed phases for $\text{Sc}_{0.38}\text{Ga}_{0.62}\text{N}$ and $\text{Sc}_{0.5}\text{Ga}_{0.5}\text{N}$ are confirmed from the selected area diffraction patterns, however the signal from the cubic phase appears much higher than the wurtzite and this suggests the cubic phase is dominant in these films with high Sc concentration. Regarding the hexagonal wurtzite phase, the E_2^H phonon mode of GaN is found at $569 \pm 1 \text{ cm}^{-1}$, close to the literature value of 568 cm^{-1} [48–50], and the peak of this mode shifts to $559 \pm 1 \text{ cm}^{-1}$ as the Sc content increases to $x = 0.26$, as expected for alloy films in which an increase in the concentration of a relatively heavier element occurs. Although in-plane stress is another possible factor causing the redshift of the Raman peak, the $\text{Sc}_x\text{Ga}_{1-x}\text{N}$ films are believed to be relaxed as the film thicknesses are larger than the critical thickness suggested by Zhang et al. [51] and the in-plane lattice parameter of the $\text{Sc}_x\text{Ga}_{1-x}\text{N}$ films differs significantly from that of the underlying GaN buffer layers. On the other hand, the E_2^H phonon mode peaks became asymmetric and reduce in intensity as the Sc content increases, this is believed to be a result of the presence of basal stacking faults, which has been reported in Ref. [52].

4 Conclusions In conclusion, under the metal-rich growth condition, single-phase hexagonal $\text{Sc}_x\text{Ga}_{1-x}\text{N}$ films were achieved for $0 \leq x \leq 0.26$, although some in-plane rotational misorientation is observed. The phase transition at $x = 0.26$ is consistent with theoretical predictions for $\text{Sc}_x\text{Ga}_{1-x}\text{N}$ films and significantly higher than the value of $x = 0.17$ demonstrated by Constantin et al. for plasma-assisted MBE growth of $\text{Sc}_x\text{Ga}_{1-x}\text{N}$ under nitrogen-rich conditions [26]. These results indicate that the use of metal-rich conditions can help to stabilise the wurtzite phase in $\text{Sc}_x\text{Ga}_{1-x}\text{N}$ films, thereby allowing a greater range of optical and electronic properties to be achieved in this alloy system.

Acknowledgments MAM acknowledges support through a Royal Society University Research Fellowship and through ERC Starting Grant ‘SCOPE’.

References

- [1] H. Morkoc, S. Strite, G. B. Gao, M. E. Lin, B. Sverdlov and M. Burns, *J. Appl. Phys.* **76**, 1363 (1994)
- [2] H. Angerer, D. Brunner, F. Freudenberg, O. Ambacher, M. Stutzmann, R. Hopler, T. Metzger, E. Born, G. Dollinger, A. Bergmaier, S. Karsch and H. -J. Korner, *Appl. Phys. Lett.* **71**, 1504 (1997)
- [3] S. Nakamura, T. Mukai and M. Senoh, *Appl. Phys. Lett.* **64**, 1687 (1994)
- [4] V. Yu. Davydov, A. A. Klochikhin, R. P. Seisyan, V. V. Emtsev, S. V. Ivanov, F. Bechstedt, J. Furthmuller, H. Harima, A. V. Mudryi, J. Aderhold, O. Semchinova and J. Graul, *phys. stat. sol. (b)* **229**, R1 (2002)
- [5] M. Kneissl, T. Kolbe, C. Chua, V. Kueller, N. Lobo, J. Stellmach, A. Knauer, H. Rodriguez, S. Einfeldt, Z. Yang, N. M. Johnson and M. Weyers, *Semicond. Sci. Technol.* **26** 014036 (2011)
- [6] S. Kerdsonpanya, N. V. Nong, N. Pryds, A. Zukauskaite, J. Jensen, J. Birch, J. Lu, L. Hultman, G. Wingqvist and P. Eklund, *Appl. Phys. Lett.* **99**, 232113 (2011)
- [7] H. Morkoc, S. Strite, G. B. Gao, M. E. Lin, B. Sverdlov and M. Burns, *J. Appl. Phys.* **76**, 1363 (1994)
- [8] M. A. Moram, Z. H. Barber and C. J. Humphreys, *Thin Solid Films* **516**, 8569 (2008)
- [9] J. L. Hall, M. A. Moram, A. Sanchez, S. V. Novikov, A. J. Kent, C. T. Foxon, C. J. Humphreys and R. P. Champion, *J. Cryst. Growth* **311**, 2054 (2009)
- [10] H. Al-Britthen and A. R. Smith, *Appl. Phys. Lett.* **77**, 2485 (2000)
- [11] D. Gall, I. Petrov, L. D. Madsen, J. -E. Sundgren and J. E. Green, *J. Vac. Sci. Technol. A* **16**, 2411 (1998)
- [12] S. Kerdsonpanya, B. Alling and P. Eklund, *J. Appl. Phys.* **114**, 073512 (2013)
- [13] P. V. Burmistrova, D. N. Zakharov, T. Favaloro, A. Mohammed, E. A. Stach, A. Shakouri and T. D. Sands, *J. Mater. Res.* **30**, 626 (2015)
- [14] Y. Oshima, E. G. Villora and K. Shimamura, *J. Appl. Phys.* **115**, 153508 (2014)
- [15] M. A. Moram, Y. Zhang, M. J. Kappers, Z. H. Barber and C. J. Humphreys, *Appl. Phys. Lett.* **91**, 152101 (2007)
- [16] M. A. Moram, M. J. Kappers, T. B. Joyce, P. R. Chalker, Z. H. Barber and C. J. Humphreys, *J. Cryst. Growth* **308**, 302 (2007)
- [17] M. A. Moram, C. F. Johnston, M. J. Kappers, C. J. Humphreys, *J. Cryst. Growth* **311**, 329 (2009)
- [18] S. W. King, R. J. Nemanich and R. F. Davis, *Appl. Phys. Lett.* **105**, 081606 (2014)
- [19] S. Zerroug, F. Ali Sahraoui and N. Bouarissa, *J. Appl. Phys.* **103**, 063510 (2008)
- [20] S. Kerdsonpanya, B. Alling and P. Eklund, *J. Appl. Phys.* **114**, 073512 (2013)
- [21] C. Constantin, M. B. Haider, D. Ingarm, A. R. Smith, N. Sandler, K. Sun and P. Ordjon, *J. Appl. Phys.* **98**, 123501 (2005)
- [22] S. Zhang, D. Holec, W. Y. Fu, C. J. Humphreys, and M. A. Moram, *J. Appl. Phys.* **114**, 133510 (2013)
- [23] N. Farrer and L. Bellaiche, *Phys. Rev. B* **66**, 201203 (2002)
- [24] R. Engel-Herber and M. Henini (editor), *Molecular Beam Epitaxy: From research to mass production* (Elsevier Inc., USA, 2013) p. 421
- [25] M. E. Little and M. E. Kordes, *Appl. Phys. Lett.* **78**, 2891 (2001)

- [26]C. Constantin, H. Al-Britthen, M. B. Haider, D. Ingram and A. R. Smith, *Phys. Rev. B* **70**, 193309 (2004)
- [27]M. A. Moram, Y. Zhang, T. B. Joyce, D. Holec, P. R. Chalker, P. H. Mayrhofer, M. J. Kappers and C. J. Humphreys, *J. Appl. Phys.* **106**, 113533 (2009)
- [28]S. M. Knoll, S. K. Rhode, S. Zhang, T. B. Joyce and M. A. Moram, *Appl. Phys. Lett.* **104**, 101906 (2014)
- [29]E. J. Tarsa, B. Heying, X. H. WU, P. Fini, S. P. DenBaars and J. S. Speck, *J. Appl. Phys.* **82**, 5472 (1997)
- [30]B. Heying, R. Averbeck, L. F. Chen, E. Haus, H. Riechert and J. S. Speck, *J. Appl. Phys.* **88**, 1855 (2000)
- [31]R. Held, D. E. Crawford, A. M. Johnston, A. M. Dabiran and P. I. Cohen, *J. Electron. Mater.* **26**, 272 (1997)
- [32]A. R. Smith, V. Ramachandran, R. M. Feenstra, D. W. Greve, A. Ptak, T. Myers, W. Sarney, L. Salamanca-Riba, M. Shin and M. Skowronski, *MRS Internet. J. Nitride Semicond. Res.* **3**, 12 (1998)
- [33]H. C. L. Tsui, L. E. Goff, N. P. Barradas, E. Alves, S. Pereira, R. Palgrave, R. J. Davies, H. E. Beere, I. Farrer, C. A. Nicoll, D. A. Ritchie, M. A. Moram, Composition measurement of epitaxial $\text{Sc}_x\text{Ga}_{1-x}\text{N}$ films (submitted to *J. Cryst. Growth*)
- [34]N. P. Barradas, E. Alves, C. Jeyes and M. Tosaki, *Nucl. Instrum. Methods Phys. Res. B* **247**, 381 (2006)
- [35]I. Horcas, R. Fernández, J. M. Gómez-Rodríguez, J. Colchero, J. Gómez-Herrero and A. M. Baro, *Rev. Sci. Instrum.* **78**, 013705 (2007)
- [36]M. A. Moram, T. B. Joyce, P. R. Chalker, Z. H. Barber and C. J. Humphreys, *Appl. Surf. Sci.* **252**, 8385 (2006)
- [37]N. Newman, *J. Cryst. Growth* **178**, 102 (1997)
- [38]M. B. Haider, C. Constantin, H. Al-Britthen, H. Yang, E. Trifan, D. Ingram, A. R. Smith, C. V. Kelly and Y. Ijiri, *J. Appl. Phys.* **93**, 5274 (2003)
- [39]V. Kirchner, R. Ebel, H. Heinke, S. Einfeldt, D. Hommel, H. Selke and P. L. Ryder, *Mat. Sci. Eng. B* **59**, 47 (1999)
- [40]H. Y. Shin, C. W. Yang, S. H. Jung and J. B. Yoo, *J. Korean Phys. Soc.* **42**, S403 (2003)
- [41]S. W. King, R. F. Davis and R. J. Nemanich, *J. Vac. Sci. Technol. A* **32**, 061504 (2014)
- [42]S. Ruvimov, Z. Liliental-Weber, J. Washburn, H. Amano, I. Akasaki and M. Koike, *Mat. Res. Soc. Symp. Proc.* **482**, 387 (1998)
- [43]M. Leszczynsk, H. Teisseyre, T. Suski, I. Grzegory, M. Bockowski, J. Jun, S. Porowski, K. Pakula, J. M. Baranowski, C. T. Foxon and T. S. Cheng, *Appl. Phys. Lett.* **69**, 73 (1996)
- [44]M. A. Moram, Z. H. Barber and C. J. Humphreys, *J. Appl. Phys.* **102**, 023505 (2007)
- [45]M. A. Moram and M. E. Vickers, *Rep. Prog. Phys.* **72**, 036502 (2009)
- [46]Z. Gu, J. H. Edgar, J. Pomeroy, M. Kuball and D. W. Coffey, *J. Mater. Sci. Mater. Electron.* **15**, 555 (2009)
- [47]B. Saha, G. Naik, V. P. Drachev, A. Boltasseva, E. E. Marinero and T. D. Sands, *J. Appl. Phys.* **114**, 063519 (2013)
- [48]Z. C. Fen, W. Wang, S. J. Chua, P. X. Zhang, K. P. J. Williams and G. D. Pitt, *J. Raman Spectrosc.* **32**, 840 (2001)
- [49]V. Yu. Davydov, Yu. E. Kitaev, I. N. Goncharuk, A. N. Smirnov, J. Graul, O. Semchinova, D. Uffmann, M. B. Smirnov, A. P. Mirgorodsky and R. A. Evarestov, *Phys. Rev. B* **58**, 12899 (1998)
- [50]T. Azuhata, T. Sota, K. Suzuki and S. Nakamura, *J. Phys.: Condens. Matter* **7**, L129 (1995)

- [51] S. Zhang, W. Y. Fu, D. Holec, C. J. Humphreys and M. A. Moram, *J. Appl. Phys.* **114**, 243516 (2013)
- [52] H. C. L. Tsui, L. E. Goff, S. K. Rhode, S. Pereira, H. E. Beere, I. Farrer, C. A. Nicoll, D. A. Ritchie and M. A. Moram, *Appl. Phys. Lett.* **106**, 132103 (2015)